Transmit/Passive Beamforming Design for Multi-IRS Assisted Cell-Free MIMO Networks

Kewei Wang, Nan Qi, *Senior Member, IEEE*, Xin Guan, Qingjiang Shi, *Senior Member, IEEE*, Ming Xiao, *Senior Member, IEEE*, Shi Jin, *Senior Member, IEEE*, and Kai-Kit Wong, *Fellow, IEEE*

***Abstract*—For beyond fifth-generation and sixth-generation communication, intelligent reflecting surface (IRS)/reconfigurable intelligent surface, and cell-free networks have been proposed as revolutionary technologies, which could significantly improve the connection quality and coverage to meet future communication demands for extremely massive connectivity and high reliability. In this article, a transmit/passive beamforming strategy for multi-IRS assisted cell-free multi-input–multi-output network is proposed to maximize the weighted sum-rate (WSR). Specifically, for passive beamforming of IRS, an elementwise block coordinate descent framework is applied to efficiently solve the unit-modulus constraints and reduce computation complexity greatly. Note that, every variable in our proposed algorithm can be updated with closed-form solutions and our algorithm can be applied with distributed implementation. Both analytical and simulation results demonstrate that, while guaranteeing superiority in WSR performance and information interaction cost, the proposed scheme outperforms the benchmark algorithms with closed-form solutions significantly in terms of complexity cost.**

***Index Terms*—Beamforming, cell-free network, elementwise block coordinate descent (BCD), intelligent reflecting surface (IRS)/reconfigurable intelligent surface (RIS), weighted sum-rate (WSR) maximization.**

Manuscript received 15 January 2023; revised 8 June 2023; accepted 11 August 2023. This work was supported in part by the Postgraduate Research and Practice Innovation Program of NUAA under Grant xcxjh20220401, in part by the Natural Science Foundation of China through Key Project under Grant 61931011, in part by the National Natural Science Foundation of China under Grant 62271253, Grant 61801218, and Grant 62071223, in part by the open research fund of National Mobile Communications Research Laboratory, Southeast University under Grant 2023D09, and in part by the Fundamental Research Funds for the Central Universities under Grant NS2023018. *(Corresponding author: Nan Qi.)*

Kewei Wang is with the College of Electronic and Information Engineering, Nanjing University of Aeronautics and Astronautics, Nanjing 210016, China (e-mail: wangkw@nuaa.edu.cn).

Nan Qi is with the School of Electrical Engineering of KTH, Royal Institute of Technology, 100 44 Stockholm, Sweden, and also with the National Mobile Communications Research Laboratory, Southeast University, Nanjing 211189, China (e-mail: nanqi.commun@gmail.com).

Xin Guan is with the School of Software Engineering, Tongji University, Shanghai 200092, China (e-mail: guanxin@tongji.edu.cn).

Qingjiang Shi is with the School of Software Engineering, Tongji University, Shanghai 200092, China, and also with the Shenzhen Research Institute of Big Data, Shenzhen 518172, China (e-mail: qing.j.shi@gmail.com).

Ming Xiao is with the School of Electrical Engineering of KTH, Royal Institute of Technology, 100 44 Stockholm, Sweden (e-mail: mingx@kth.se).

Shi Jin is with the National Mobile Communications Research Laboratory, Southeast University, Nanjing 211189, China (e-mail: jinshi@seu.edu.cn).

Kai-Kit Wong is with the Department of Electronic and Electrical Engineering, University College London, WC1E 7JE London, U.K. (e-mail: kai-kit.wong@ucl.ac.uk).

Digital Object Identifier 10.1109/JSYST.2023.3307556

I. Introduction

CELL-FREE network is considered to be a promising technology to address the demands, such as high spectral efficiency, low latency, and high reliability in future beyond fifth-generation and sixth-generation communication [1]. Compared with traditional cellular networks, in which the users (UEs) located at the cell boundaries suffer from severe intercell interference and path loss so that the system performance may be limited, in cell-free networks, all base stations (BSs) collaborate with each other and serve all the UEs simultaneously without cell boundaries. The system performance can be enhanced in cell-free multi-input–multi-output (MIMO) systems, since they inherit the benefits of the distributed MIMO and network MIMO architectures, and the users are closer to the BSs [2]. It has been shown that the cell-free MIMO system outperforms the small-cell system [3]. Intelligent reflecting surface (IRS) is also a revolutionizing technology, which is comprised of several low-cost and low-energy-consumption elements, each of which can controllably change the phase or amplitude of the incident signals [4], [5]. This enables IRS to change the wireless channels in order to accomplish extremely massive connectivity and higher quality of service (QoS) [6], [7] for UEs, such as improving physical layer security and enhancing QoS of UEs at the dead zone and cell edge. [8], [9], [10]. As a result, integrating IRS and cell-free networks is considered to be greatly promising in increasing the capacity of wireless networks [11].

Weighted sum-rate (WSR) maximization is an important research topic in IRS-assisted communication networks [12], [13], [14]. Introducing IRS into network optimization will cause coupling between variables in objective functions and nonconvex unit-modulus phase-shift constraints, which is challenging to solve. Especially for the unit-modulus constraints, traditional methods, e.g., semidefinite relaxation (SDR) [15], [16], [17], [18], [19], [20], [21], and successive convex approximation [22] will cause a high complexity and is hard for practical implementation. Moreover, they can hardly get closed-form solutions and be applied in a distributed framework, which may decrease computation and equipment burden. In [23], a decentralized algorithm was proposed for the WSR problem in multi-IRS and multi-UE cell-free MIMO system, the majorization–minimization (MM) method was applied to eliminate the unit-modulus constraints, which can obtain a closed-form solution. However, determining the upper bound of the objective function involves the eigenvalue decomposition,

which may bring a higher complexity when the dimension of the matrix is large and can be replaced by algorithms with a lower complexity while achieving similar performance.

Based on the above observations, this article proposes a low-complexity, low-interaction, distributed joint optimization strategy of transmit and passive beamforming design for WSR maximization. The main contributions are summarized as follows.

1) We propose a block coordinate descent (BCD)-based low-complexity transmit/passive beamforming method for multi-IRS assisted cell-free MIMO networks, by jointly optimizing the transmit beamforming at the BSs and passive beamforming of IRSs, the WSR is maximized.
2) Different from many existing algorithms [13], [14], [15], [22], each variable in our proposed algorithm is updated with a closed-form solution instead of solving a convex problem. Especially, for passive beamforming of IRS, to achieve low complexity, we apply the elementwise BCD framework and treat every entry of phase-shift matrices as a block instead of updating the whole matrix simultaneously. Compared with several benchmark algorithms, while guaranteeing similar system performance in WSR, our proposed scheme reduces the complexity greatly. To the best of author's knowledge, the complexity of the proposed algorithm is the lowest compared with other schemes.
3) We consider WSR maximization in multi-IRS assisted multi-UE cell-free networks, which is a more general scenario. Compared with most published work [12], [13], [15], [22], the cell-free network can be seen as an expansion to traditional cellular networks and increases the coupling of variables, thus more mathematical processing is required. Moreover, considering practical factors, such as space limitation, it will be more flexible to deploy multiple IRSs to cooperate, while most works focused on the single-IRS scenario, which are the special cases of our general scenario. Note that considering multiple cooperating IRS causes the objective function to be more complex and coupled.
4) The proposed algorithm can be applied for distributed implementation. A distributed framework between BS and UE, and BS and BS is designed to reduce the equipment burden, and the amount of interaction for computation is low.

II. System Model

As depicted in Fig. 1, we consider a typical scenario, in the downlink of IRS-aided cell-free MIMO system, B BSs serve K UEs with R IRSs simultaneously. We assume that every BS and UE is equipped with N_t transmit antennas and a single receive antenna, respectively. Moreover, we assume that IRSs can only change the phase of the incident signal, the element number of each IRS is N, and the phase shift matrix of IRS r is denoted by $\mathbf{\Phi}_r = \mathrm{diag}(\mathrm{e}^{j\phi_{r,1}}, \mathrm{e}^{j\phi_{r,2}}, \ldots, \mathrm{e}^{j\phi_{r,N}}) \in \mathbb{C}^{N\times N}$, where $\mathrm{e}^{j\phi_{r,n}}$ is the phase shift coefficient of the nth element in IRS r. Let $\mathbf{G}_{b,r} \in \mathbb{C}^{N\times N_t}$, $\mathbf{h}_{b,k}^H \in \mathbb{C}^{1\times N_t}$, and $\mathbf{v}_{r,k}^H \in \mathbb{C}^{1\times N}$ be

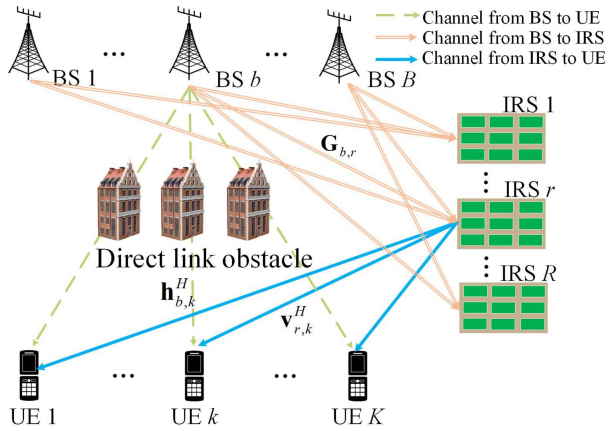

Fig. 1. Multi-IRS assisted cell-free network system.

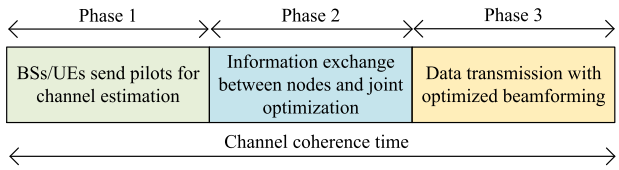

Fig. 2. Practical transmission protocol for IRS.

the channel between BS b to IRS r, channel between BS b to UE k, and the channel between IRS r to UE k, respectively.

Furthermore, in order to obtain perfect channel state information (CSI), we applied the transmission protocol in [24] of time-division duplexing system, in which additional sensing devices need to be deployed on IRSs to endow them with sensing capability for channel estimation and the procedures are as follows. As shown in Fig. 2, each channel coherence period is divided into three different phases. In phase 1, the BSs and UEs send pilot signals in downlink and uplink transmission, respectively, to estimate the direct-link channels between them, which is the same as the scenario without IRSs, whereas the IRSs operate as the sensing mode to receive signals from BSs and UEs in order to estimate the CSI from them. In phase 2, CSI can be exchanged between the IRS controller and BSs via an independent wireless/wired backhaul link, making the interaction and implementation of the proposed distributed algorithm feasible. On the basis of information interaction, the transmit beamforming of BSs and the passive beamforming of IRSs are jointly optimized. Finally, in phase 3, IRSs turn to the transmission mode with optimized phase-shift matrices to improve the performance of communication, whereas the BSs send signals with optimized transmit beamforming. In practice, the BS-IRS links have longer channel coherence time than BS-UE and IRS-UE links due to the mobility of UEs, and have few scatters due to the high altitude of BSs and IRSs generally. As a result, the BS-IRS links can be seen as quasistatic and estimated by utilizing channel properties, such as low-rank and sparsity [24]. It is worth noting that, there is a tradeoff between the accuracy of the channel estimation and the system complexity since the number of sensors and the resolution of analog-to-digital converter for sensors will affect the accuracy of channel estimation greatly.

The equivalent channel between BS b and UE k can be written as[1]

$$\begin{aligned}\hat{\mathbf{h}}_{b,k}^H &= \mathbf{h}_{b,k}^H + \sum_{r=1}^{R} \mathbf{v}_{r,k}^H \mathbf{\Phi}_r^H \mathbf{G}_{b,r} \\ &= \mathbf{h}_{b,k}^H + \boldsymbol{\theta}^H \mathbf{V}_k^H \mathbf{G}_b \end{aligned} \tag{1}$$

where $\boldsymbol{\theta} = [\mathrm{diag}(\mathbf{\Phi}_1)^T, \mathrm{diag}(\mathbf{\Phi}_2)^T, \ldots, \mathrm{diag}(\mathbf{\Phi}_R)^T]^T \in \mathbb{C}^{NR\times 1}$, $\mathbf{V}_k = \mathrm{diag}([\mathbf{v}_{1,k}^T, \ldots, \mathbf{v}_{R,k}^T]) \in \mathbb{C}^{NR\times NR}$, and $\mathbf{G}_b = [\mathbf{G}_{b,1}^T, \ldots, \mathbf{G}_{b,R}^T]^T \in \mathbb{C}^{NR\times N_t}$. We then define that $s_k \in \mathbb{C}^{1\times 1}$ is the symbol sent to UE k by all the BSs, where $\mathbb{E}_{s_k}\{s_k s_k^H\} = 1\,\forall k$. Let $\mathbf{f}_{b,k} \in \mathbb{C}^{N_t\times 1}$ be the transmit beamforming vector of BS b to UE k, and let $n_k \sim \mathcal{CN}(0, \sigma_k^2)$ represent the additive white Gaussian noise at UE k's receiver. Thus, the signal received by UE k is

$$\begin{aligned} y_k &= \sum_{b=1}^{B}\sum_{j=1}^{K} \hat{\mathbf{h}}_{b,k}^H \mathbf{f}_{b,j} s_j + n_k \\ &= \underbrace{\sum_{b=1}^{B} \hat{\mathbf{h}}_{b,k}^H \mathbf{f}_{b,k} s_k}_{\text{Desired signal}} + \underbrace{\sum_{j=1, j\neq k}^{K}\sum_{b=1}^{B} \hat{\mathbf{h}}_{b,k}^H \mathbf{f}_{b,j} s_j}_{\text{Interference}} + \underbrace{n_k}_{\text{noise}}. \end{aligned} \tag{2}$$

The signal-to-interference-plus-noise ratio (SINR) of UE k can be written as

$$\Gamma_k = \frac{\left|\sum_{b=1}^{B} \hat{\mathbf{h}}_{b,k}^H \mathbf{f}_{b,k}\right|^2}{\sum_{j=1, j\neq k}^{K} \left|\sum_{b=1}^{B} \hat{\mathbf{h}}_{b,k}^H \mathbf{f}_{b,j}\right|^2 + \sigma_k^2}. \tag{3}$$

We aim to maximize the WSR of all UEs by jointly optimizing transmit beamforming of BSs and passive beamforming of IRSs. The optimization problem can be formulated as follows:

$$\begin{aligned} \underset{\mathbf{F},\boldsymbol{\theta}}{\text{maximize}} \quad & \sum_{k=1}^{K} \alpha_k \log\left(1+\Gamma_k\right) \\ \text{subject to} \quad & \sum_{k=1}^{K} \|\mathbf{f}_{b,k}\|_2^2 \leqslant P_b \forall b \\ & |\theta_n| = 1\,\forall n \end{aligned} \tag{4}$$

where $\mathbf{F} = \{\mathbf{f}_{b,k}\}\,\forall b, k$ is the set of beamforming vectors for all the BSs, and P_b and θ_n are the maximum transmit power in BS b, and the nth element in $\boldsymbol{\theta}$, respectively. α_k is the weight coefficient of UE k, indicating its importance level, a larger α_k means a higher priority of UE k.

Although the power constraints are convex, the problem is still a nonconvex problem due to the coupling of variables in the objective function and the unit modulus constraints, which is challenging to solve.

III. Transmit/Passive Beamforming Design

Since the variables in constraints are separable, the BCD method is applied in our algorithm. In this section, we will propose a BCD-based, distributed, low-complexity, joint optimization algorithm for WSR maximization. In every iteration, we first fix $\boldsymbol{\theta}$ to optimize $\mathbf{F}$, then we calculate $\boldsymbol{\theta}$ at given $\mathbf{F}$.

A. Transmit Beamforming Design

For fixed $\boldsymbol{\theta}$, let $u_k^* \in \mathbb{C}^{1\times 1}$ be the decoding coefficient of UE k, the estimated signal is $\hat{s}_k = u_k^* y_k$. Then, the mean-square error (MSE) coefficient of UE k can be written as

$$\begin{aligned} e_k &= \mathbb{E}_{s,\mathbf{n}}\left[\left(\hat{s}_k - s_k\right)\left(\hat{s}_k - s_k\right)^H\right] \\ &= 1 - 2\,\mathrm{Re}\left\{u_k \sum_{b=1}^{B} \mathbf{f}_{b,k}^H \hat{\mathbf{h}}_{b,k}\right\} + \sigma_k^2 |u_k|^2 \\ &\quad + |u_k|^2 \left[\sum_{j=1}^{K}\left|\sum_{b=1}^{B} \hat{\mathbf{h}}_{b,k}^H \mathbf{f}_{b,j}\right|^2\right]. \end{aligned} \tag{5}$$

By using the minimize mean-square error (MMSE) receiver, the problem (4) with respect to $\mathbf{F}$ can be equivalently converted to a weighted MMSE (WMMSE) problem [25], which is

$$\begin{aligned} \underset{\mathbf{w},\mathbf{u},\mathbf{F}}{\text{minimize}} \quad & \sum_{k=1}^{K} \alpha_k \left(w_k e_k - \log w_k\right) \\ \text{subject to} \quad & \sum_{k=1}^{K} \|\mathbf{f}_{b,k}\|_2^2 \leqslant P_b \forall b \end{aligned} \tag{6}$$

where $\mathbf{w} = \{w_k\}\forall k$, $\mathbf{u} = \{u_k\}\forall k$ stand for the set of auxiliary weighted variables and decoding coefficients. Since (6) is convex with respect to each variable in $\mathbf{w}$, $\mathbf{u}$, and $\mathbf{F}$, we use BCD method to solve (6).

For the decoding coefficient u_k, let $\frac{\partial \sum_{i=1}^{k} e_i}{\partial u_k} = 0$, we can obtain the optimal MMSE receiver u_k^{opt}, that is

$$u_k^{\mathrm{opt}} = \frac{\sum_{b=1}^{B}\left(\hat{\mathbf{h}}_{b,k}^H \mathbf{f}_{b,k}\right)}{\sum_{j=1}^{K}\left(\sum_{b=1}^{B} \hat{\mathbf{h}}_{b,k}^H \mathbf{f}_{b,j}\right)\left(\sum_{b=1}^{B} \mathbf{f}_{b,j}^H \hat{\mathbf{h}}_{b,k}\right) + \sigma_k^2}. \tag{7}$$

For the auxiliary weighted variable w_k, according to the optimal condition to the objective function in (6), we have its optimal value as

$$w_k^{\mathrm{opt}} = e_k^{-1}. \tag{8}$$

When w_k and $u_k\forall k$ are fixed, the WMMSE problem can be rewritten as follows:

$$\begin{aligned} \underset{\mathbf{F}}{\text{minimize}} \quad & \sum_{k=1}^{K} \alpha_k w_k e_k \\ \text{subject to} \quad & \sum_{k=1}^{K} \|\mathbf{f}_{b,k}\|_2^2 \leqslant P_b \forall b. \end{aligned} \tag{9}$$

Note that problem (9) is a convex quadratic constrained quadratic programming optimization problem and has a monotonic gradient function, which can be solved by the bisection method. Specially, the Lagrangian function can be written as (10), shown at the bottom of the next page, where λ_b and C_1 are, respectively, the dual variable respect to BS b and constant irrelevant to $\mathbf{f}_{b,k}$.

[1]Since the signals reflected between IRSs twice and more times are weak due to the large path loss in multiple hops channel, which can be ignored [14].

According to the optimal condition, $\mathbf{f}_{b,k}$ is a function of λ_b, as shown in (11), shown at the bottom of the page. By finding the dual variable, we can calculate the beamforming vector $\mathbf{f}_{b,k}$.

It is obvious that $\sum_{k=1}^{K} \mathrm{Tr}(\mathbf{f}_{b,k}\mathbf{f}_{b,k}^H) = P_b \forall b$, which can be written as

$$\mathrm{Tr}\left[\left(\mathbf{\Lambda}_b + \lambda_b \mathbf{I}\right)^{-2} \mathbf{\Omega}_b\right] = P_b \tag{12}$$

where

$$\mathbf{\Omega}_b = \sum_{k=1}^{K} \mathbf{D}_b^H \mathbf{x}_{b,k}\mathbf{x}_{b,k}^H \mathbf{D}_b \tag{13}$$

$$\mathbf{x}_{b,k} = \alpha_k w_k u_k \hat{\mathbf{h}}_{b,k} - \sum_{i=1}^{K} \alpha_i w_i \left|u_i\right|^2 \left(\sum_{b'=1, b'\neq b}^{B} \hat{\mathbf{h}}_{b',i}^H \mathbf{f}_{b',k}\right) \hat{\mathbf{h}}_{b,i}. \tag{14}$$

We assume that $\mathbf{D}_b \mathbf{\Lambda}_b \mathbf{D}_b^H = \sum_{i=1}^{K} \alpha_i w_i |u_i|^2 \hat{\mathbf{h}}_{b,i}\hat{\mathbf{h}}_{b,i}^H$ is the eigenvalue decomposition. Consequently, we have

$$\sum_{m=1}^{N_t} \frac{\left[\mathbf{\Omega}_b\right]_{m,m}}{\left(\left[\mathbf{\Lambda}_b\right]_{m,m} + \lambda_b\right)^2} = P_b. \tag{15}$$

The left-hand side of (15) is monotonically decreasing with respect to λ_b. Thus, λ_b can be found by using the bisection method.

B. Passive Beamforming Design

When $\mathbf{F}$ is fixed, $\mathbf{u}$ and $\mathbf{w}$ can be derived according to (7) and (8). Then the WMMSE problem with respect to $\boldsymbol{\theta}$ can be rewritten as follows:

$$\begin{aligned} &\underset{\boldsymbol{\theta}}{\text{minimize}} \sum_{k=1}^{K} \alpha_k w_k e_k \\ &\text{subject to } \left|\theta_n\right| = 1 \forall n. \end{aligned} \tag{16}$$

According to (1) and (5), problem (16) is actually a quadratic optimization problem, which is nonconvex due to the unit-modulus constraints, and can be rewritten as

$$\begin{aligned} &\underset{\boldsymbol{\theta}}{\text{minimize}} \;\; f(\boldsymbol{\theta}) \triangleq \boldsymbol{\theta}^H \mathbf{Z} \boldsymbol{\theta} - 2\,\mathrm{Re}\left\{\boldsymbol{\theta}^H \mathbf{q}\right\} + C_2 \\ &\text{subject to } \left|\theta_n\right| = 1 \forall n \end{aligned} \tag{17}$$

where C_2 is a constant irrelevant with respect to $\boldsymbol{\theta}$. $\mathbf{Z}$ and $\mathbf{q}$ are shown in (18) and (19), respectively, which are also irrelevant to $\boldsymbol{\theta}$.

$$\mathbf{Z} = \sum_{k=1}^{K} \alpha_k w_k \left|u_k\right|^2 \times \left[\sum_{j=1}^{K} \left(\sum_{b=1}^{B} \mathbf{V}_k^H \mathbf{G}_b \mathbf{f}_{b,j}\right)\left(\sum_{b=1}^{B} \mathbf{f}_{b,j}^H \mathbf{G}_b^H \mathbf{V}_k\right)\right] \tag{18}$$

$$\mathbf{q} = \sum_{k=1}^{K} \left[\alpha_k w_k u_k^* \left(\sum_{b=1}^{B} \mathbf{V}_k^H \mathbf{G}_b \mathbf{f}_{b,k}\right)\right] - \sum_{k=1}^{K} \alpha_k w_k \left|u_k\right|^2 \times \left[\sum_{j=1}^{K} \left(\sum_{b=1}^{B} \mathbf{V}_k^H \mathbf{G}_b \mathbf{f}_{b,j}\right)\left(\sum_{b=1}^{B} \mathbf{f}_{b,j}^H \mathbf{h}_{b,k}\right)\right] \tag{19}$$

Finding an upper bound with the MM method by eigenvalue decomposition may cause a higher complexity and a lower convergence rate. Instead, we use the elementwise BCD algorithm to solve (17), especially, in each step we treat one entry of $\boldsymbol{\theta}$ as a block and optimize that block while fixing other blocks. Note that since the constraints with respect to every entry of $\boldsymbol{\theta}$ are separate, convergence to stationary solutions can be guaranteed [26], [27], [28]. Without loss of generality, we consider problem (17) with respect to the n-entry of $\boldsymbol{\theta}$, i.e., θ_n as follows:

$$\begin{aligned} &\underset{\theta_n}{\text{minimize}} f(\boldsymbol{\theta}) \\ &\text{subject to } \left|\theta_n\right| = 1. \end{aligned} \tag{20}$$

Since we have fixed $\theta_{n'} \forall n' \neq n$, it can be observed that the function $f(\boldsymbol{\theta})$ with respect to θ_n is actually a quadratic function in the form of $g(\theta_n) \triangleq \mu|\theta_n|^2 - 2\,\mathrm{Re}\{\kappa^*\theta_n\} + C_3$, where μ is a real number, κ is a complex number, and C_3 is a constant and irrelevant to θ_n. Considering that $|\theta_n| = 1$, problem (20) can be reduced into

$$\begin{aligned} &\underset{\theta_n}{\text{maximize}}\, \mathrm{Re}\left\{\kappa^* \theta_n\right\} \\ &\text{subject to } \left|\theta_n\right| = 1. \end{aligned} \tag{21}$$

Obviously, the closed-form solution for problem (21) is $\theta_n^{\text{opt}} = \kappa/|\kappa|$, i.e., the same phase was achieved by θ_n and κ. Consequently, the closed-form solution of θ_n can be achieved only when κ is determined.

$$\mathcal{L}\left(\mathbf{f}_{b,k}, \lambda_b\right) = \mathbf{f}_{b,k}^H \left(\sum_{i=1}^{K} \alpha_i w_i \left|u_i\right|^2 \hat{\mathbf{h}}_{b,i}\hat{\mathbf{h}}_{b,i}^H + \lambda_b \mathbf{I}\right) \mathbf{f}_{b,k} + \left[\sum_{i=1}^{K} \alpha_i w_i \left|u_i\right|^2 \left(\sum_{b'=1, b'\neq b}^{B} \mathbf{f}_{b',k}^H \hat{\mathbf{h}}_{b',i}\right) \hat{\mathbf{h}}_{b,i}^H - \alpha_k w_k u_k^* \hat{\mathbf{h}}_{b,k}^H\right] \mathbf{f}_{b,k} + \mathbf{f}_{b,k}^H \left[\sum_{i=1}^{K} \alpha_i w_i \left|u_i\right|^2 \left(\sum_{b'=1, b'\neq b}^{B} \hat{\mathbf{h}}_{b',i}^H \mathbf{f}_{b',k}\right) \hat{\mathbf{h}}_{b,i} - \alpha_k w_k u_k \hat{\mathbf{h}}_{b,k}\right] + C_1 \tag{10}$$

$$\mathbf{f}_{b,k}^{\text{opt}}\left(\lambda_b\right) = \left(\sum_{i=1}^{K} \alpha_i w_i \left|u_i\right|^2 \hat{\mathbf{h}}_{b,i}\hat{\mathbf{h}}_{b,i}^H + \lambda_b \mathbf{I}\right)^{-1} \left[\alpha_k w_k u_k \hat{\mathbf{h}}_{b,k} - \sum_{i=1}^{K} \alpha_i w_i \left|u_i\right|^2 \left(\sum_{b'=1, b'\neq b}^{B} \hat{\mathbf{h}}_{b',i}^H \mathbf{f}_{b',k}\right) \hat{\mathbf{h}}_{b,i}\right] \tag{11}$$

Algorithm 1: Elementwise BCD in Proposed Algorithm.

Update $\mathbf{Z}$ according to (18).
Update $\mathbf{q}$ according to (19).
Update $\mathbf{p}$ by $\mathbf{p} = \mathbf{Z}\boldsymbol{\theta}$.
For $n = 1 : NR$
  $\kappa = [\mathbf{Z}]_{n,n}\tilde{\theta_n} - [\mathbf{p}]_n + [\mathbf{q}]_n$
  $\theta_n^{\text{opt}} = \kappa/|\kappa|$
  $\mathbf{p} = \mathbf{p} + ((\theta_n^{\text{opt}} - \theta_n)\mathbf{Z}(:,n)\mathbf{1}_{NR}^H)$
  $\theta_n = \theta_n^{\text{opt}}$
End for
Return $\boldsymbol{\theta}$

To calculate κ, complex gradients are calculated from two different perspectives. On one hand, the complex gradient of $f(\boldsymbol{\theta})$ with respect to $\boldsymbol{\theta}$ can be calculated as [29]

$$\left.\frac{\partial f(\boldsymbol{\theta})}{\partial \boldsymbol{\theta}^*}\right|_{\boldsymbol{\theta}=\tilde{\boldsymbol{\theta}}} = \frac{1}{2}(\mathbf{Z}\tilde{\boldsymbol{\theta}} - \mathbf{q}). \tag{22}$$

On the other hand, since $f(\boldsymbol{\theta})$ is a quadratic function of θ_n, the complex derivative of $f(\boldsymbol{\theta})$ with respect to θ_n can be calculated as [29]

$$\left.\frac{\partial f(\theta_n)}{\partial \theta_n^*}\right|_{\theta_n=\tilde{\theta_n}} = \frac{1}{2}(\rho\tilde{\theta_n} - \kappa). \tag{23}$$

Since the complex gradient is unique, by defining $[\cdot]_{m,n}$ representing the m,nth entry of the matrix and $[\cdot]_n$ representing the nth entry of the vector, from (22) and (23), we can derive the conclusion that

$$\left[\mathbf{Z}\tilde{\boldsymbol{\theta}} - \mathbf{q}\right]_n = \rho\tilde{\theta_n} - \kappa. \tag{24}$$

Considering $[\mathbf{Z}\tilde{\boldsymbol{\theta}} - \mathbf{q}]_n = [\mathbf{Z}\tilde{\boldsymbol{\theta}}]_n - [\mathbf{q}]_n$, the coefficient of $\tilde{\theta_n}$ is $[\mathbf{Z}]_{n,n}$. By comparing the two sides of (24) with the coefficient of $\tilde{\theta_n}$, we have $\rho\tilde{\theta_n} = [\mathbf{Z}]_{n,n}\tilde{\theta_n}$. As a result, by expanding ρ in (24), and we can update κ by

$$\kappa = [\mathbf{Z}]_{n,n}\,\tilde{\theta_n} - \left[\mathbf{Z}\tilde{\boldsymbol{\theta}}\right]_n + [\mathbf{q}]_n\,. \tag{25}$$

The above steps of elementwise BCD in our algorithm are summarized in Algorithm 1, where the update of $\mathbf{p}$ means that $\mathbf{Z}\boldsymbol{\theta}$ is changing with θ_n updating.

Therefore, the overall algorithm is summarized in Algorithm 2. It is worth noting that the WMMSE and elementwise approach are actually BCD methods [25], [26], and the convergence can be guaranteed.

Note that instead of solving a convex problem by standard solvers, such as Mosek and CVX [14], [15], [22], every step in our proposed algorithm has a closed-form solution, which leads to lower complexity and is beneficial for hardware deployment.

IV. Distributed Implementation and Numerical Results

In this section, we will provide the distributed implementation and numerical analysis of the proposed algorithm.

Algorithm 2: Low-Complexity BCD for Problem (4).

Initialize $\mathbf{f}_{b,k}, \boldsymbol{\Phi}_r, \mathbf{v}_{r,k}^H, \mathbf{G}_{b,r}, \mathbf{h}_{b,k}^H, \alpha_k, P_b, \forall b,k,r$, with $\sum_{k=1}^K \text{Tr}(\mathbf{f}_{b,k}\mathbf{f}_{b,k}^H) = P_b, \forall b$.
Update $\hat{\mathbf{h}}_{b,k}^H, \forall b,k$ according to (1).
Repeat
  Update u_k and $w_k, \forall k$ according to (7) and (8).
  For $b = 1 : B$
    Update $\boldsymbol{\Lambda}_b$ and $\boldsymbol{\Omega}_b$ according to (12)–(14).
    Update λ_b with bisection method.
    Update $\mathbf{f}_{b,k}, \forall k$ according to (11).
    Update $\mathbf{Z}$ and $\mathbf{q}$ according to (18) and (19).
    Update $\mathbf{p}$ by $\mathbf{p} = \mathbf{Z}\boldsymbol{\theta}$.
    For $n = 1 : NR$
      Update θ_n by solving (21).
    End for
    Update $\hat{\mathbf{h}}_{b,k}^H, \forall b,k$ according to (1).
  End for
Until convergence

TABLE I
Main Complexity Comparison of Five Algorithms

Method	Complexity of algorithms
Proposed algorithm	$\mathcal{O}\left(I_1\left(BKN_t^3 + BN^2R^2N_t + BN^2R^2\right)\right)$
Alternating direction method of multipliers (ADMM) in [21]	$\mathcal{O}\left(I_2\left(BKN_t^3 + BN^2R^2 + BN^3R^3\right)\right)$
Closed-form FP in [28] with MM	$\mathcal{O}\left(I_3\left(BKN_t^3 + BN^2R^2N_t + BN^3R^3\right)\right)$
WMMSE with MM	$\mathcal{O}\left(I_4\left(BKN_t^3 + BN^2R^2N_t + BN^3R^3\right)\right)$
Direct FP in [29] with SDR in [30]	$\mathcal{O}\left(I_5\left((NR+1)^{4.5} + (BKN_t)^{3.5}\right)\right)$

A. Complexity Analysis

In Algorithm 2, the computational complexity consists of two parts: calculation on UEs and BSs. For each UE, according to (7) and (8), the main complexity is the dot product of two N_t-dimensional vectors and the division of a real number, which leads to a low complexity and can be neglected in the proposed algorithm. For any BS b, in the transmit beamforming, the complexity is caused by eigenvalue decomposition before (15), calculation of the diagonal elements of $\boldsymbol{\Omega}$ in (15), bisection method to obtain λ_b, and the inverse operation in (11) for K UEs. The eigenvalue decomposition and matrix inverse both cause a calculation complexity of $\mathcal{O}(N_t^3)$, calculation of the diagonal elements in Hermitian matrix $\boldsymbol{\Omega}_b$ causes a complexity of $\mathcal{O}(N_t^2)$, and the bisection method causes a complexity of $\mathcal{O}(\log_2(L_0/\epsilon))$, where ϵ is the target precision and L_0 is the initial search length interval of bisection method. For passive beamforming, the complexity includes calculation of $\mathbf{Z}$, calculation of $\mathbf{p}$, and update of $\mathbf{p}$, which cause the complexity of $\mathcal{O}(N^2R^2N_t + NRN_t)$, $\mathcal{O}(N^2R^2N_t + NRN_t)$, and $\mathcal{O}(NR)$, respectively. Consequently, considering B BSs and NR blocks in Algorithm 1, the above complexity is $\mathcal{O}(I_1(BN_t^3 + BN_t^2 + BKN_t^3 + B\log_2(L_0/\epsilon) + 2B(N^2R^2N_t + NRN_t) + BN^2R^2))$.

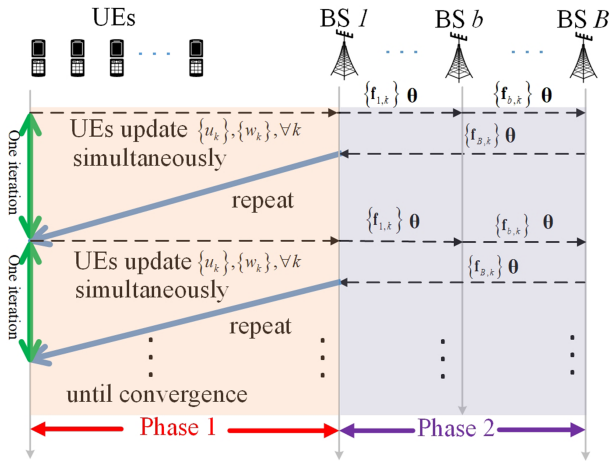

Fig. 3. Information interaction order of proposed distributed algorithm.

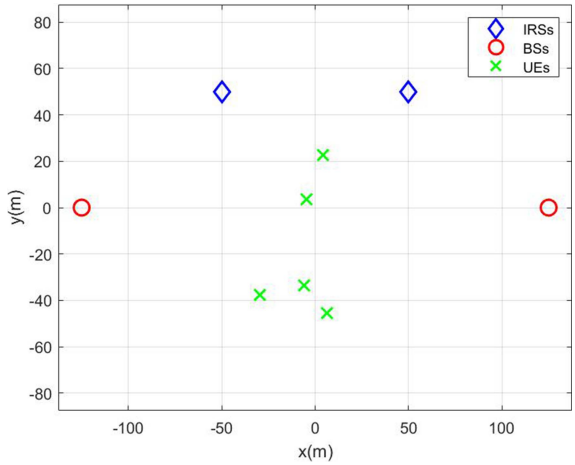

Fig. 4. Location of BSs, IRSs, and UEs, where the location of UEs is generated randomly.

TABLE II
TOTAL REQUIRED INTERACTIONS IN EACH ITERATION

Method	Interaction
Proposed algorithm	$2K + B\left(KN_t + NR\right)$
ADMM in [21]	$B\left(2K^2 + NRB\right)$
FP in [29] with MM	$B\left(KN_t + NR + 2K\right)$
WMMSE with MM (distributed)	$2K + B\left(KN_t + NR\right)$

In Table I, we summarize the complexity of several different algorithms. For simplicity, we only compare the highest order of complexity [23], and assume that I_1, I_2, I_3, I_4, and I_5 represent the required iteration numbers for convergence. Note that the first four algorithms are all executed in distributed ways and all have closed-form solutions. As given in Table I, the complexity of the proposed algorithm is the lowest. Since usually the element number N of IRSs is large, it is worth noting that the complexity is cut down by many orders of magnitude.

B. Distributed Implementation and Message Overhead

For the distributed algorithms, complexity and message overheads are two important factors, the complexity is analyzed in Section IV-A. Thus, in this Section IV-B, we will analyze the distributed implementation and message overhead of Algorithm 2.

As shown in Fig. 3, in each iteration the distributed implementation of the proposed algorithm can be divided into two phases. In phase 1, every UE updates u_ks and w_ks according to (7) and (8), respectively, and broadcasts them to BSs. After that, in phase 2, BSs sequentially update their beamforming vectors and $\boldsymbol{\theta}$, then broadcasts to other BSs and UEs.

Note that $u_k \in \mathbb{C}^{1\times 1}\forall k$, $w_k \in \mathbb{R}^{1\times 1}\forall k$, $\mathbf{f}_{b,k} \in \mathbb{C}^{N_t\times 1}\forall k$, and $\boldsymbol{\theta} \in \mathbb{C}^{NR\times 1}$, in each iteration, the required information interaction between BSs and UEs is in phase 1, when the UEs, respectively, broadcast totally $2K$ 1-D complex number u_ks and w_ks, the required information interaction of BSs includes the number of K N_t-dimensional beamforming vector $\mathbf{f}_{b,1},\ldots,\mathbf{f}_{b,K}$ and one NR-dimensional phase-shift vector $\boldsymbol{\theta}$ in phase 2. Therefore, the total required information interaction is $2K + B(KN_t + NR)$, as given in Table II. The proposed algorithm has the lowest information interaction in the following algorithm as well as distributed WMMSE, but it is worth mentioning that our proposed algorithm has a lower complexity than it.

C. Parameters and Channel Model

We assume that the BSs are located on a circle centered at (0,0) with radius R_c, and the UEs were generated by random location in this circle. For simplicity and without loss of generality, we set $B = 2, R = 2, K = 5, R_c = 125$ m, and $\alpha_k = 1\forall k$ and assume that the BSs are located at (R_c,0) and ($-R_c$,0), IRSs are located at (50,50) and ($-$50,50), as shown in Fig. 4. The height of BS, IRS, and UE is set to be 30, 10, and 1.5 m, respectively [12].

1) Large-Scale Fading Model: We refer to the large-scale fading model in [1] and [2], where the path loss, shadow fading, and block probability of direct link are considered.

a) Path loss model: For the path loss, we use the three-slope model, which is generally considered in cell-free networks. The large-scale path loss in dB is given by

$$\mathrm{PL} = \begin{cases} L - \varepsilon \log_{10} d, & \text{if } d > d_1 \\ L - 15\log_{10} d_1 - 20\log_{10} d, & \text{if } d_0 < d < d_1 \\ L - 15\log_{10} d_1 - 20\log_{10} d_0, & \text{if } d < d_0 \end{cases} \tag{26}$$

where L is the path loss at the reference distance of 1 m, ε is the path loss exponent for different channels, d is the distance from the transmitter to the receiver, and d_0 and d_1 are the distance thresholds for the three slopes. We set $L = -30$ dB, $\sigma_k^2 = -80$ dBm$\forall k$ [14], the path-loss exponent ϵ of BS-UE link non-line-of-sight (NLoS) and BS-IRS, IRS-UE link line-of-sight (LoS) is set to be 3.75 and 2.2, respectively, and we assume that $d_0 = 10$ m and $d_1 = 50$ m [1].

b) Shadow fading: Considering the direct-link obstacles, the large-scale fading coefficient $\tilde{\beta}_{b,k}$ of BS-UE links can be modeled as

$$\tilde{\beta}_{b,k} = \mathrm{PL}_{b,k} \cdot 10^{\frac{\sigma_{\mathrm{sh}} \cdot z}{10}} \forall b,k \tag{27}$$

where $10^{\frac{\sigma_{\mathrm{sh}} \cdot z}{10}}$ represents the shadow fading with the standard deviation σ_{sh}, and $z \sim \mathcal{N}(0,1)$ [1].

c) Block probability of direct-link: Considering the block probability, the large-scale fading coefficient for the direct-link

TABLE III
SIMULATION PARAMETER SETTINGS

Parameters	Value
Number of BSs B	2
Number of IRSs R	2
Number of UEs K	5
Weight of all UEs $\alpha_k\ \forall k$	1
2-D coordinate of BSs	(-125,0), (0,125)
2-D coordinate of IRSs	(-50,50), (50,50)
Height of BSs, IRSs, and UEs (m)	30, 10, and 1.5
Reference distance (m)	1
Path loss at the reference distance L (dB)	-30
Distance thresholds for the three slopes model (m)	10, 50
Path-loss exponent for LoS link $\varepsilon^{\mathrm{LoS}}$	2.2
Path-loss exponent for nLoS link $\varepsilon^{n\,\mathrm{LoS}}$	3.75
Rician factor γ	3
Noise power (dBm)	-80
Number of receive antenna N_r	1

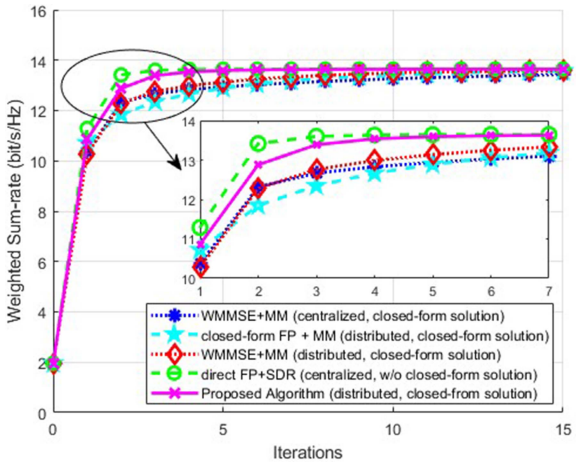

Fig. 5. Convergence of algorithms when $N_t = 4, N = 40, P_b = 30$ dBm, $\sigma_{\mathrm{sh}} = 8$ dB, and $\tilde{p} = 0$.

channels is formulated as follows:

$$\beta_{b,k} = \tilde{\beta}_{b,k} a_{b,k} \forall b, k \tag{28}$$

where the binary variables $a_{b,k}$ means whether the link is blocked, and can be defined as

$$a_{b,k} = \begin{cases} 0, \text{with probability of } \tilde{p} \\ 1, \text{with probability of } 1 - \tilde{p} \end{cases} \tag{29}$$

where $\tilde{p} \in [0, 1]$ accounts for that the direct link is not blocked [2].

2) Small-Scale Fading Model: For the BS-UE link, we set the small-scale fading to be Rayleigh fading, whereas the Rician fading for the BS-IRS, IRS-UE link, which can be written as

$$\tilde{\mathbf{H}} = \sqrt{\frac{\gamma}{\gamma+1}} \tilde{\mathbf{H}}^{\mathrm{LoS}} + \sqrt{\frac{1}{\gamma+1}} \tilde{\mathbf{H}}^{\mathrm{NLoS}} \tag{30}$$

where the Rician factor γ is set to be 3, and $\tilde{\mathbf{H}}^{\mathrm{LoS}}$ and $\tilde{\mathbf{H}}^{\mathrm{NLoS}}$ are the deterministic LoS and the NLoS components, respectively [12].

The variables in Table III are the parameters used for performance analysis in the simulation, unless otherwise specified.

D. Numerical Results and Performance Analysis

Fig. 5 shows the convergence performance of several algorithms when fixing $N_t = 4, N = 40, P_b = 30$ dBm, $\sigma_{\mathrm{sh}} = 8$ dB, $\tilde{p} = 0$, and the parameters in different algorithms are initialized to the same value. In every iteration, the transmit beamforming of all the BSs and phase-shift matrices of all the IRSs are updated. It can be shown in Fig. 5 that, all the algorithms in the figure have good convergence performance and finally converge to a stationary point. Moreover, the convergence rate of the proposed algorithm is higher than the other benchmark algorithms, which have closed-form solutions. Although the direct-fractional programming (FP) with the widely used SDR method converges in fewer iterations, it is worth noting that the transmit beamforming and passive beamforming in that algorithm are solved by standard convex solvers, which will cause a higher computation complexity and the closed-form solution is hard to achieve.

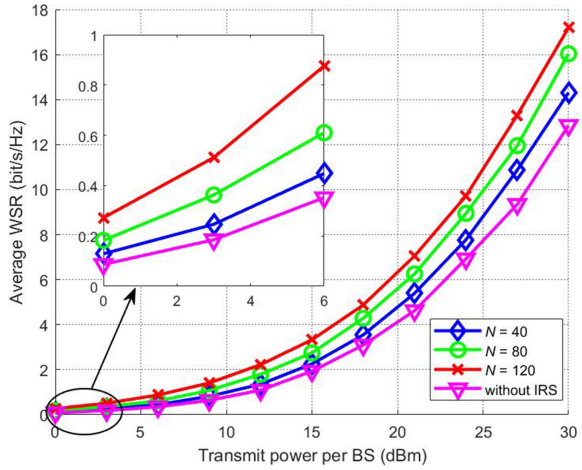

Fig. 6. Average WSR versus transmit power when $N_t = 4, \sigma_{\mathrm{sh}} = 8$ dB, and $\tilde{p} = 0$.

Fig. 6 presents the average WSR, which varies with the transmit power and the number of elements in IRS. We fix $N_t = 4, \sigma_{\mathrm{sh}} = 8$ dB, $\tilde{p} = 0$, and every curve is averaged over 100 channel realizations. It is obvious that the more transmit power the BSs use, the higher the average WSR the UEs can obtain. Besides, since the system gain brought by introducing IRSs scales with the element number in IRSs [24], increasing the number of elements in IRSs can improve the performance of the system.

Fig. 7 demonstrates that the average WSR varies with the transmit power and the number of transmit antennas in BSs. In this figure, we set $N = 40, \sigma_{\mathrm{sh}} = 8$ dB, $\tilde{p} = 0$, and every curve is averaged by 100 channel realizations. Similar to Fig. 6, higher average WSR can be achieved by higher power consumption by each BS. Moreover, to improve WSR, the number of transmit antennas of BSs need to be increased. However, as the dimension of beamforming vector increases, the computational complexity will increase accordingly.

Fig. 8 illustrates the performance comparison of several relevant schemes, including direct FP with widely used SDR [15], [31], closed-form FP with MM in [23], [30], WMMSE with MM in [12], and maximum radio transmission (MRT) [33], each algorithm adopts the same initialization values and every curve is averaged by 100 algorithm execution. Since closed-form FP has a strong link with WMMSE [30], when applying the same

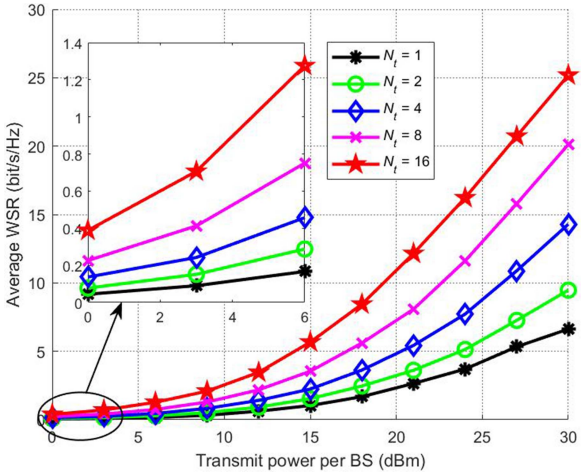

Fig. 7. Average WSR versus transmit power when $N = 40, \sigma_{\text{sh}} = 8$ dB, and $\tilde{p} = 0$.

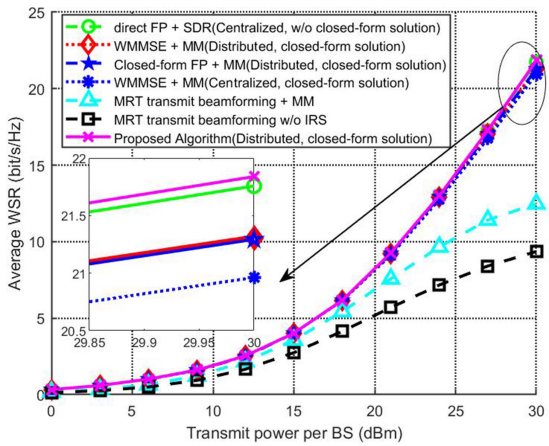

Fig. 8. Performance of different algorithms when $N = 80, N_t = 8, \sigma_{\text{sh}} = 8$ dB, and $\tilde{p} = 0$.

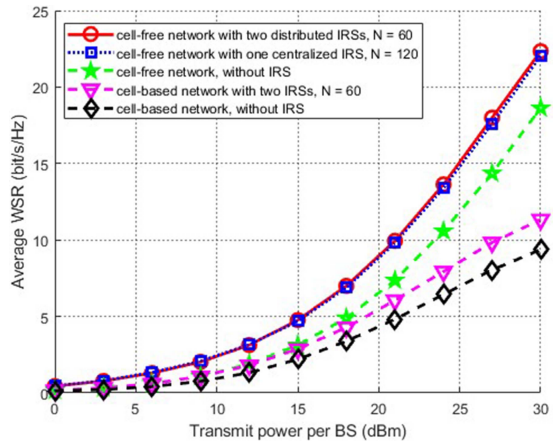

Fig. 9. Performance comparison with different deployment strategies when $N_t = 8, \sigma_{\text{sh}} = 8$ dB, and $\tilde{p} = 0$.

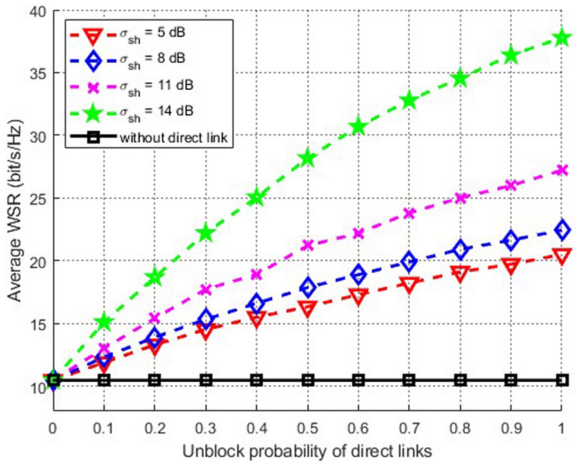

Fig. 10. Average WSR versus unblock probability of direct links under different levels of obstacles (shadow fading) when $N_t = 8, P_b = 30$ dBm $\forall b$, and $N = 120$.

passive beamforming strategy MM, these two algorithms have a very similar performance in distributed framework. It is interesting that the distributed WMMSE with MM algorithm slightly outperforms the centralized WMMSE with MM algorithm, that is because in distributed framework, every BS updates $\boldsymbol{\theta}$ for one time in each iteration, compared with that in centralized frameworks, in which in each iteration, the central node updates $\boldsymbol{\theta}$ for one time, it will provide more precise information for transmit beamforming. It can be shown from Fig. 8 that our proposed algorithm outperformed the traditional MRT beamforming strategy (even with MM passive beamforming) and acquired about the same performance as the other benchmark algorithms, note that the computation complexity in our proposed algorithm is the lowest.

Fig. 9 demonstrates the performance comparison of different deployment strategies. We fix $N_t = 8, \sigma_{\text{sh}} = 8$ dB, $\tilde{p} = 0$, and every curve is averaged by 100 channel realizations. For the deployment of IRS, we applied two strategies: centralized deployment and distributed deployment. For the distributed IRS deployment strategy, similar with that in Fig. 4, we assume there are two IRSs, and $N = 60$ for each IRS. For the centralized IRS deployment strategy, we assume that there is only one large-scale IRS with $N = 120$, while the location of BSs, UEs, and other parameters remain unchanged. For the cell-based network, each cell is equipped with one IRS with $N = 60$ with other system parameters unchanged. Compared with centralized IRS deployment, in distributed deployment, the distance between IRS-BS, and IRS-UE can be shortened, and thus the path loss is reduced [34], so higher system rates can be obtained, that is the reason why in Fig. 9 the distributed strategy slightly outperformed the centralized one, and in practice, the distributed deployment is more flexible since it may not always be possible to deploy a large-scale IRS due to space limits. However, considering the information exchange brought by multi-IRS, it is hard to judge which deployment strategy is better [24]. Since in cell-free networks, BSs serve UEs cooperatively and simultaneously with no cell boundaries so that the spectral resource can be utilized more efficiently [1], [2], [3], it can be seen from Fig. 9 that the average WSR of cell-free networks is

higher than that in cell-based networks with the same transmit power per BS.

Fig. 10 shows how the average WSR varies with the unblock probability of direct links and the standard deviation of shadow fading, every curve is averaged by 100 channel realizations. It can be concluded from Fig. 10 that the average WSR increases with the unblock probability of direct links, when $\tilde{p} = 0$ (direct links are completely blocked) the performance is the worst. Moreover, the level of direct obstacles has an impact on the average WSR. When the deviation of shadow fading σ_{sh} increases (lower obstacle level), the system performance is able to improve.

V. Conclusion

In this article, a low-complexity, low-interaction, closed-form solution, distributed beamforming strategy for multi-IRS assisted cell-free MIMO network was proposed so that the WSR can be maximized. Both analytical and simulation results demonstrated that, while guaranteeing superiority in WSR performance and information interaction cost, the proposed scheme outperforms the benchmark distributed algorithms significantly in terms of complexity cost.

References

[1] H. Q. Ngo, A. Ashikhmin, H. Yang, E. G. Larsson, and T. L. Marzetta, "Cell-free massive MIMO versus small cells," *IEEE Trans. Wireless Commun.*, vol. 16, no. 3, pp. 1834–1850, Mar. 2017.

[2] T. Van Chien, H. Q. Ngo, S. Chatzinotas, M. Di Renzo, and B. Ottersten, "Reconfigurable intelligent surface-assisted cell-free massive MIMO systems over spatially-correlated channels," *IEEE Trans. Wireless Commun.*, vol. 21, no. 7, pp. 5106–5128, Jul. 2022.

[3] S. Elhoushy, M. Ibrahim, and W. Hamouda, "Cell-free massive MIMO: A survey," *IEEE Commun. Surv. Tut.*, vol. 24, no. 1, pp. 492–523, Jan.–Mar. 2022.

[4] C. Pan et al., "An overview of signal processing techniques for RIS/IRS-aided wireless systems," *IEEE J. Sel. Topics Signal Process.*, vol. 16, no. 5, pp. 883–917, Aug. 2022.

[5] Q. Zhu, Y. Gao, Y. Xiao, M. Xiao, and S. Mumtaz, "Intelligent reflecting surface aided wireless networks: Dynamic user access and system sum-rate maximization," *IEEE Trans. Commun.*, vol. 70, no. 4, pp. 2870–2881, Apr. 2022.

[6] N. Qi, M. Xiao, T. A. Tsiftsis, M. Skoglund, P. L. Cao, and L. Li, "Energy-efficient cooperative network coding with joint relay scheduling and power allocation," *IEEE Trans. Commun.*, vol. 64, no. 11, pp. 4506–4519, Nov. 2016.

[7] N. Qi, M. Xiao, T. A. Tsiftsis, L. Zhang, M. Skoglund, and H. Zhang, "Efficient coded cooperative networks with energy harvesting and transferring," *IEEE Trans. Wireless Commun.*, vol. 16, no. 10, pp. 6335–6349, Oct. 2017.

[8] Q. Wu and R. Zhang, "Towards smart and reconfigurable environment: Intelligent reflecting surface aided wireless network," *IEEE Commun. Mag.*, vol. 58, no. 1, pp. 106–112, Jan. 2020.

[9] Y. Han, W. Tang, S. Jin, C.-K. Wen, and X. Ma, "Large intelligent surface-assisted wireless communication exploiting statistical CSI," *IEEE Trans. Veh. Technol.*, vol. 68, no. 8, pp. 8238–8242, Aug. 2019.

[10] W. Tang et al., "Wireless communications with reconfigurable intelligent surface: Path loss modeling and experimental measurement," *IEEE Trans. Wireless Commun.*, vol. 20, no. 1, pp. 421–439, Jan. 2021.

[11] Y. Zhang, B. Di, H. Zhang, J. Lin, Y. Li, and L. Song, "Reconfigurable intelligent surface aided cell-free MIMO communications," *IEEE Wireless Commun. Lett.*, vol. 10, no. 4, pp. 775–779, Apr. 2021.

[12] C. Pan et al., "Multicell MIMO communications relying on intelligent reflecting surfaces," *IEEE Trans. Wireless Commun.*, vol. 19, no. 8, pp. 5218–5233, Aug. 2020.

[13] H. Guo, Y. C. Liang, J. Chen, and E. G. Larsson, "Weighted sum-rate maximization for reconfigurable intelligent surface aided wireless networks," *IEEE Trans. Wireless Commun.*, vol. 19, no. 5, pp. 3064–3076, May 2020.

[14] Z. Zhang and L. Dai, "A joint precoding framework for wideband reconfigurable intelligent surface-aided cell-free network," *IEEE Trans. Signal Process.*, vol. 69, pp. 4085–4101, Jun. 2021, doi: 10.1109/TSP.2021.3088755.

[15] Q. Wu and R. Zhang, "Intelligent reflecting surface enhanced wireless network via joint active and passive beamforming," *IEEE Trans. Wireless Commun.*, vol. 18, no. 11, pp. 5394–5409, Nov. 2019.

[16] C. Kai, W. Ding, and W. Huang, "Max-min fairness in IRS-aided MISO broadcast channel via joint transmit and reflective beamforming," in *Proc. GLOBECOM IEEE Glob. Commun. Conf.*, 2020, pp. 1–6.

[17] H. Xie, J. Xu, and Y.-F. Liu, "Max-min fairness in IRS-aided multi-cell MISO systems with joint transmit and reflective beamforming," *IEEE Trans. Wireless Commun.*, vol. 20, no. 2, pp. 1379–1393, Feb. 2021.

[18] M. W. Shabir, T. N. Nguyen, J. Mirza, B. Ali, and M. A. Javed, "Transmit and reflect beamforming for max-min SINR in IRS-aided MIMO vehicular networks," *IEEE Trans. Intell. Transp. Syst.*, vol. 24, no. 1, pp. 1099–1105, Jan. 2023.

[19] W. Huang, W. Ding, C. Kai, Y. Yi, and Y. Huang, "Joint placement and beamforming design for IRS-enhanced multiuser MISO systems," *IEEE Trans. Commun.*, vol. 70, no. 10, pp. 6678–6692, Oct. 2022.

[20] W. Wu et al., "Joint sensing and transmission optimization for IRS-assisted cognitive radio networks," *IEEE Trans. Wireless Commun.*, vol. 22, no. 9, pp. 5941–5956, Sep. 2023, doi: 10.1109/TWC.2023.3238684.

[21] L. Ge, H. Zhang, and J. Wang, "Joint placement and beamforming design in multi-UAV-IRS assisted multiuser communication," in *Proc. IEEE Glob. Commun. Conf.*, 2021, pp. 1–6.

[22] X. Yu, D. Xu, D. W. K. Ng, and R. Schober, "Power-efficient resource allocation for multiuser MISO systems via intelligent reflecting surfaces," in *Proc. IEEE Glob. Commun. Conf.*, 2020, pp. 1–6.

[23] S. Huang, Y. Ye, M. Xiao, H. V. Poor, and M. Skoglund, "Decentralized beamforming design for intelligent reflecting surface-enhanced cell-free networks," *IEEE Wireless Commun. Lett.*, vol. 10, no. 3, pp. 673–677, Mar. 2021.

[24] Q. Wu, S. Zhang, B. Zheng, C. You, and R. Zhang, "Intelligent reflecting surface-aided wireless communications: A tutorial," *IEEE Trans. Commun.*, vol. 69, no. 5, pp. 3313–3351, May 2021.

[25] Q. Shi, M. Razaviyayn, Z.-Q. Luo, and C. He, "An iteratively weighted MMSE approach to distributed sum-utility maximization for a MIMO interfering broadcast channel," *IEEE Trans. Signal Process.*, vol. 59, no. 9, pp. 4331–4340, Sep. 2011.

[26] Q. Shi and M. Hong, "Spectral efficiency optimization for millimeter wave multiuser MIMO systems," *IEEE J. Sel. Topics Signal Process.*, vol. 12, no. 3, pp. 455–468, Jun. 2018.

[27] X. Yu, D. Xu, and R. Schober, "Enabling secure wireless communications via intelligent reflecting surfaces," in *Proc. IEEE Glob. Commun. Conf.*, 2019, pp. 1–6.

[28] D. P. Bertsekas, "Nonlinear programming," *J. Oper. Res. Soc.*, vol. 48, no. 3, 1997, Art. no. 334.

[29] K. B. Petersen and M. S. Pedersen, "The matrix cookbook," *Tech. Univ. Denmark*, vol. 7, no. 15, 2008, pp. 24–27.

[30] K. Shen and W. Yu, "Fractional programming for communication systems–Part II: Uplink scheduling via matching," *IEEE Trans. Signal Process.*, vol. 66, no. 10, pp. 2631–2644, May 2018.

[31] K. Shen and W. Yu, "Fractional programming for communication systems–Part I: Power control and beamforming," *IEEE Trans. Signal Process.*, vol. 66, no. 10, pp. 2616–2630, May 2018.

[32] Z. Q. Luo, W. K. Ma, M. C. So, Y. Ye, and S. Zhang, "Semidefinite relaxation of quadratic optimization problems," *IEEE Signal Process. Mag.*, vol. 27, no. 3, pp. 20–34, May 2010.

[33] T. K. Y. Lo, "Maximum ratio transmission," *IEEE Trans. Commun.*, vol. 47, no. 10, pp. 1458–1461, Oct. 1999.

[34] E. Shi et al., "Wireless energy transfer in RIS-aided cell-free massive MIMO systems: Opportunities and challenges," *IEEE Commun. Mag.*, vol. 60, no. 3, pp. 26–32, Mar. 2022.

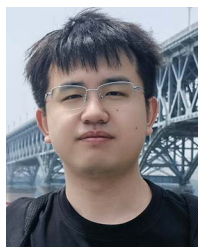

Kewei Wang received the B.S. degree in information engineering in 2021 from the Nanjing University of Aeronautics and Astronautics, Nanjing, China, where he is currently working toward the M.S. degree in electronic and information engineering with the College of Electronic and Information Engineering.

His research interests include intelligent reflecting surface, cell-free networks, MIMO wireless communications, and convex optimization.

Xin Guan received the B.S. and M.S. degrees in communication engineering from the Nanjing University of Aeronautics and Astronautics, Nanjing, China, in 2017 and 2020, respectively. He is currently working toward the Ph.D. degree in software engineering with Tongji University, Shanghai, China.

His research interests include MIMO wireless communications, UAV wireless networks, convex optimization, and reinforcement learning.

Qingjiang Shi (Senior Member, IEEE) received the Ph.D. degree in electronic engineering from Shanghai Jiao Tong University, Shanghai, China, in 2011.

From 2009 to 2010, he visited Prof. Z.-Q. (Tom) Luo's Research Group, the University of Minnesota, Twin Cities, Minneapolis, MN, USA. In 2011, he was a Research Scientist with Bell Labs, China. Since 2012, he has been with the School of Information and Science Technology, Zhejiang Sci-Tech University, Hangzhou, China. From 2016 to 2017, he was a Research Fellow with Iowa State University, Ames, IA, USA. Since 2018, he has been a Full Professor with the School of Software Engineering, Tongji University, Shanghai, China. He is also with the Shenzhen Research Institute of Big Data. He has authored or coauthored more than 60 IEEE journals and filed about 30 national patents. His research interests include algorithm design and analysis with applications in machine learning, signal processing, and wireless networks.

Dr. Shi was an Associate Editor for IEEE TRANSACTIONS ON SIGNAL PROCESSING. In 2018, he was the recipient of the golden medal at the 46th International Exhibition of Inventions of Geneva. He was also the recipient of the First Prize of Science and Technology Award from China Institute of Communications in 2018, the National Excellent Doctoral Dissertation Nomination Award in 2013, the Shanghai Excellent Doctorial Dissertation Award in 2012, and the Best Paper Award from the IEEE PIMRC'09 conference.

Ming Xiao (Senior Member, IEEE) received the bachelor's and master's degrees in engineering from the University of Electronic Science and Technology of China, Chengdu, China, in 1997 and 2002, respectively, and the Ph.D. degree in communication engineering from the Chalmers University of Technology, Goöteborg, Sweden, in 2007.

From 1997 to 1999, he was a Network and Software Engineer with ChinaTelecom. From 2000 to 2002, he was with the SiChuan communications administration. Since November 2007, he has been with the Department of Information Science and Engineering, School of Electrical Engineering and Computer Science, KTH Royal Institute of Technology, Stockholm, Sweden, where he is currently an Associate Professor.

Dr. Xiao was an Editor of IEEE TRANSACTIONS ON COMMUNICATIONS from 2012 to 2017, IEEE COMMUNICATIONS LETTERS (Senior Editor, since January 2015), and IEEE WIRELESS COMMUNICATIONS LETTERS from 2012 to 2016, and has been an Editor of the IEEE TRANSACTIONS ON WIRELESS COMMUNICATIONS, since 2018. He was the lead Guest Editor of IEEE JOURNAL ON SELECTED AREAS IN COMMUNICATIONS with Special Issue on "Millimeter Wave Communications for Future Mobile Networks," in 2017. Since 2019, he has been an Area Editor of IEEE Open Journal of the Communication Society.

Shi Jin (Senior Member, IEEE) received the B.S. degree in communications engineering from the Guilin University of Electronic Technology, Guilin, China, in 1996, the M.S. degree in information and communication engineering from the Nanjing University of Posts and Telecommunications, Nanjing, China, in 2003, and the Ph.D. degree in information and communications engineering from Southeast University, Nanjing, in 2007.

His research interests include space-time wireless communications, random matrix theory, information theory, intelligent communications, and reconfigurable intelligent surfaces.

Kai-Kit Wong (Fellow, IEEE) received the B.Eng., M.Phil., and Ph.D. degrees in electrical and electronic engineering from the Hong Kong University of Science and Technology, Hong Kong, in 1996, 1998, and 2001, respectively.

After graduation, he took up academic and research positions with the University of Hong Kong, Lucent Technologies, Bell-Labs, Holmdel, the Smart Antennas Research Group of Stanford University, and the University of Hull, U.K. He is the Chair in wireless communications with the Department of Electronic and Electrical Engineering, University College London, London, U.K. His research focuses on 5-G and beyond mobile communications.

Dr. Wong was a corecipient of the 2013 IEEE Signal Processing Letters Best Paper Award and the 2000 IEEE VTS Japan Chapter Award at the IEEE Vehicular Technology Conference in Japan in 2000, and a few other international Best Paper Awards. He is a Fellow of IET and is also on the editorial board of several international journals. Since 2020, he was the Editor-in-Chief of IEEE WIRELESS COMMUNICATIONS LETTERS.